Behaviour and effect of Ti_2Ni phase during processing of NiTi shape memory alloy wire from cast ingot

J. Bhagyaraj[#], K.V. Ramaiah*, C.N. Saikrishna*, S.K. Bhaumik*, Gouthama[#]

[#]Department of Materials Science and Engineering, Indian Institute of Technology, Kanpur 208 016, INDIA
*Council of Scientific and Industrial Research, Materials Science Division, CSIR-National Aerospace Laboratories, Bangalore 560 017, INDIA

Abstract

Binary NiTi alloy is one of the commercially successful shape memory alloys (SMAs). Generally, the alloy composition preferred for use of NiTi as thermal actuator is slightly Ti-rich. In the present study, vacuum arc melted alloy of 50.2Ti-Ni (at.%) composition was prepared and characterized using optical, scanning and transmission electron microscopy. Formation of second phase particles (SPPs) in the cast and their influence on development of microstructure during processing of alloy into wire form has been investigated. Results showed that the present alloy contained Ti_2Ni type SPPs in the matrix. In the cast alloy, the Ti_2Ni particles form in varying sizes (1-10μm) and shapes. During subsequent thermo-mechanical processing, these SPPs get sheared/fragmented into smaller particles with low aspect ratio. The presence of SPPs plays a significant role in refinement of the microstructure during processing of the alloy. During deformation of the alloy, the matrix phase around the SPPs experiences conditions similar to that observed in severe plastic deformation of metallic materials, leading to localized amorphisation of the matrix phase.

***Keywords*:** Shape memory; NiTi alloy; Ti_2Ni phase; amorphisation; microstructure; TEM

1. INTRODUCTION

Shape memory alloys (SMAs) are a class of functional materials which exhibit unique characteristic properties under external stimulus such as thermal, mechanical and magnetic field [1-2]. The unique properties of SMAs are superelasticity (SE) and shape memory effect (SME). Among SMAs, NiTi-base alloys find variety of applications in biomedical, aerospace and automobile industries because of their superior mechanical, functional and corrosion resistance properties [2-3]. The memory properties of NiTi-base alloys are limited to a narrow composition range which is near about its equi-atomic composition [4]. Deviation of alloy composition from this results in precipitation of second phase particles (SPPs) in the microstructure. Presence of these SPPs has been shown to alter the fatigue and functional behaviour of the alloys significantly.

The influence of composition on transformation behaviour and microstructure of NiTi alloys has been studied in literature [2,4]. It has been shown that a variation in Ni content of NiTi alloy by as small as 0.1 at.% shifts the transformation temperatures by ~10°C [5-8]. Tang [9] considered the available experimental data on transformation temperatures and thermodynamic properties of near equi-atomic NiTi alloys, and reported the variation of transition temperatures with composition through thermodynamic calculation. In NiTi phase diagram, the phase boundary for NiTi single phase on Ti-rich side is very steep and close to 50 at.% Ni, whereas on Ni-rich side,

the solubility of Ni decreases with decrease in temperature resulting in a two-phase microstructure [4]. Depending on alloy composition, various second phases such as Ti_2Ni, Ti_3Ni_4, Ni_3Ti have been reported [2,4,10] to form in the microstructure. In addition, the formation of SPPs also depends on thermo-mechanical processing history of the alloy [4].

Composition of SMAs is selected based on the envisaged applications. Generally, Ni-rich composition is chosen for superelastic applications, whereas equi-atomic or slightly Ti-rich compositions for shape memory applications. It has been reported that in either equi-atomic or slightly Ti-rich composition, Ti_2Ni phase forms during solidification of the alloy from the melt [10-13]. Also, the volume fraction of Ti_2Ni increases with increase in the Ti content of the alloy. The presence of Ti_2Ni not only alters Ni/Ti ratio of matrix phase leading to changes in transformation temperatures, but also plays an important role during secondary processing of the alloy. Although, the role of SPPs in microstructural refinement during thermo-mechanical processing of Al and Cu alloys has been well documented [14-17], such studies on NiTi SMAs have been scarce. In the present paper, the behavior of Ti_2Ni phase during secondary processing and its role on the microstructure of 50.2Ti-Ni (at.%) alloy is studied. The characterization techniques used in this study include optical microscopy (OM), scanning electron microscopy (SEM), and transmission electron microscopy (TEM).

2. EXPERIMENTAL PROCEDURE

Nominal composition of the alloy chosen for the present study was 50.2Ti-Ni (at.%). The alloy in pancake form and weighing about 500 g was prepared by non-consumable vacuum arc-melting process using tungsten electrode and water cooled copper crucible. High purity titanium sponge (99.97%) and nickel shots (99.99%) were used for preparation of the alloy. The pancake was flipped and re-melted six times to ensure melt homogeneity. The pancake was cut into rectangular bars and subjected to series of hot rolling and cold rolling operations. Two-high groove rolling mill was used for reducing the cross-section of the rectangular bars. The reduction in cross section in each pass of rolling was limited to 30%. Hot rolling was carried out at 850°C with inter-pass annealing for 10 min. Inter-pass annealing during cold rolling was carried out at 750°C for 10 min. Cold wire drawing was performed from wire rod of rectangular cross section 1.0×1.0 mm^2. During wire drawing inter-pass annealing was carried out at 650°C for 5 min. After multiple drawing processes, the final dimension of the wire of 500 μm diameter with 40% retained cold work was obtained. Samples for microstructural study were collected at different stages of processing and description of these samples is given in Table 1.

Samples for optical and SEM study were prepared using standard metallographic techniques and the microstructure was revealed by etching with 10%HF-18%HNO_3-72%CH_3COOH (in vol%) solution. For bulk metallic samples, specimens for TEM study were prepared by slicing out thin discs of 3 mm diameter and 500 μm thickness from the bulk alloy/rods by spark erosion method and they were subsequently thinned down 100 μm thickness by mechanical polishing using SiC paper. Electron transparent regions on these samples were obtained by twinjet electro-polishing using an electrolyte mixture of 30 vol.% HNO_3 and 70 vol.% methanol at -30°C using a potential of 12 V.For wire samples, a modified embedding technique was used to obtain longitudinal section thinned for observation. After embedding, the same procedure as practiced for the bulk sample was followed. Microstructural observations were carried out using FEI Tecnai G^2 U-

Twin TEM operating at 200 kV. The surface morphology of the electro-polished discs was analyzed using FEI Quanta 200 model SEM.

Table 1 Description of 50.2Ti-Ni (at.%) alloy samples used for microstructural study

Sample identification	Sample description	Cross section	Cumulative reduction (%)
AC	As-cast	~8.0 × 8.0 mm^2	Machined from pancake
HR30	Hot rolled rod	~6.7 × 6.7 mm^2	30
HR70	Hot rolled rod	~4.4 × 4.4 mm^2	70
CR80	Cold rolled rod	~2.0 × 2.0 mm^2	80 (after hot rolling)
CR95	Cold rolled rod	~1.0 × 1.0 mm^2	95 (after hot rolling)
CDW40	Cold drawn wire	500 μm diameter	40 (retained cold work)

3. RESULTS AND DISCUSSION

3.1 Second phase precipitates in as-cast alloy

Figure 1 shows the typical microstructural features of cast 50.2Ti-Ni (at.%)alloy. The optical micrograph in Fig. 1(a) shows that the microstructure consists of martensite laths of different orientation and revealed presence of SPPs, preferably located at the prior austenitic grain boundaries. This was confirmed through SEM observation (Fig. 1(b)), wherein SPPs at the grain boundaries can be clearly seen. Quantitative metallographic study showed that the volume fraction of the SPPs was in the range 0.01-0.02. On metallographically prepared sample, the morphology of SPPs showed circular to elongated shapes. The diameter of circular cross section measured in the range 0.5-1.0 μm, while the length of the SPPs measured in the range 1-10 μm. Gupta et al. [11] considered a series of NiTi alloy compositions and pointed out that Ti_2Ni showed an equiaxed morphology in the hypo-eutectoid alloys. Also, it has been well demonstrated in literature that Ti_2Ni phase fraction decreased with an increase in the Ni content.

The bright field TEM image in Fig.1(c) shows a typical SPP and its surrounding microstructural features. The sub-structure in the matrix phase surrounding the particle can be seen. Under the OM/SEM, these particles show smooth curved surface. TEM observations, however, shows fine scale sub-structural features. It can be seen that these particles have extended facets. Three such facets are shown in Fig.1(c) and these are marked as 1-1', 2-2' and 3-3'. Presence of these facets indicates that SPPs have well defined orientation relationship with the matrix phase. Although the SPPs are fairly large in size (1-10 μm in length), the faceted nature suggests that they are not fully incoherent with the matrix phase across the entire interface.

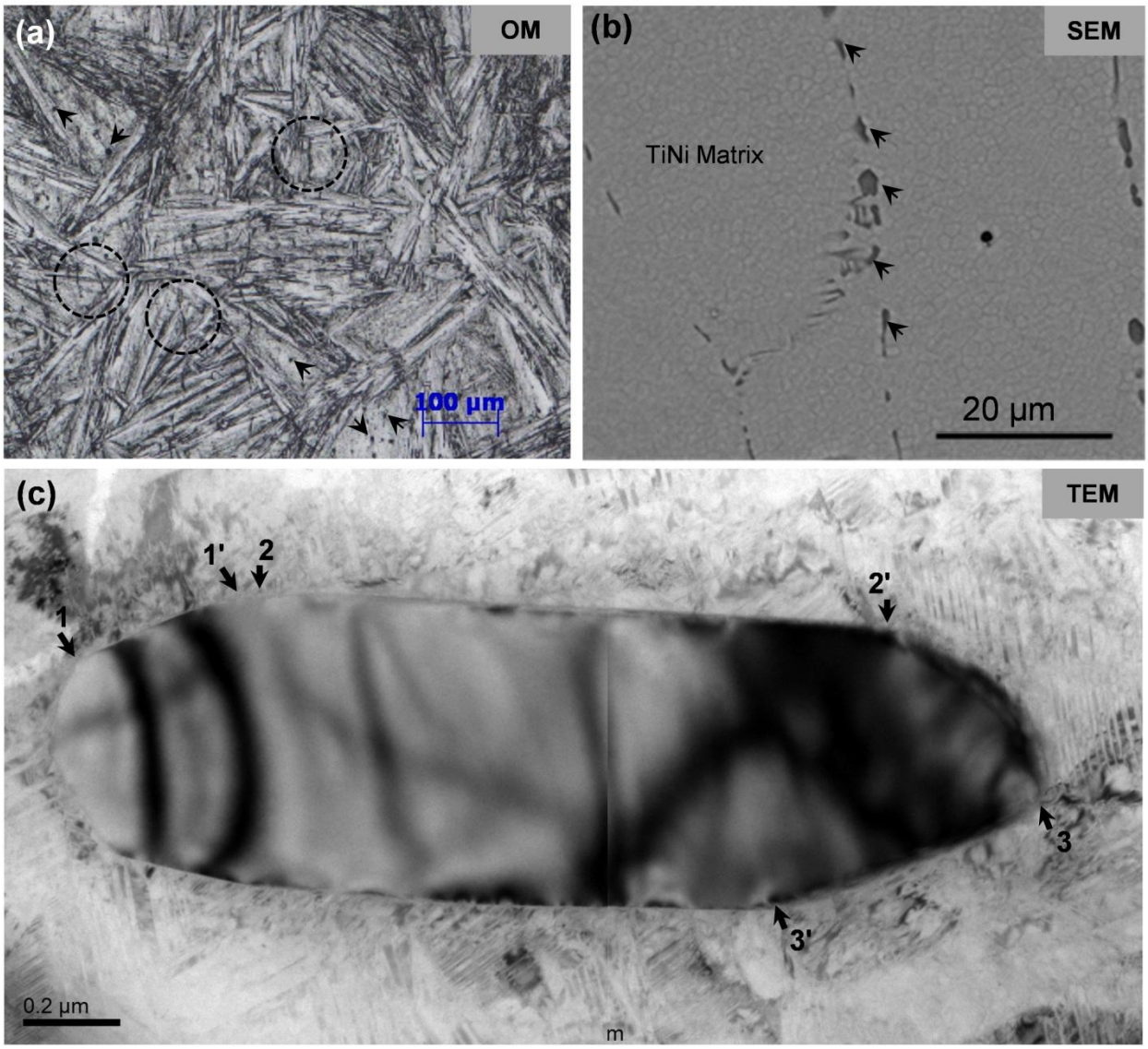

Figure 1 Micrographs illustrating morphology of SPPs in the cast alloy: (a) optical micrograph (SPPs encircled);(b) SEM micrograph showing SPPs located along the grain boundaries; and (c) bright field TEM image of an elongated SPP with extended facets along the particle-matrix interface.

Figure 2(a) shows bright field TEM image of a SPP located at the edge of thin foil specimen. The bright area on left of the particle is perforated region, while on the right is matrix phase. It can be seen that a wide region of SPP is available without any overlap of the matrix phase. Hence, it was possible to analyse the composition of SPP without any interference from matrix phase. Compositional analysis was carried out using energy dispersive spectroscopy (EDS) attachment operating with STEM mode of TEM. Figure 2(b) shows the results of a line scan covering the SPP as well as the matrix phase. The results of the quantitative analysis are given in Table 2. The matrix phase showed composition close to that of the nominal composition of the alloy. The Ti:Ni ratio in the SPP was found to be 2:1 confirming to stoichiometric Ti_2Ni phase.

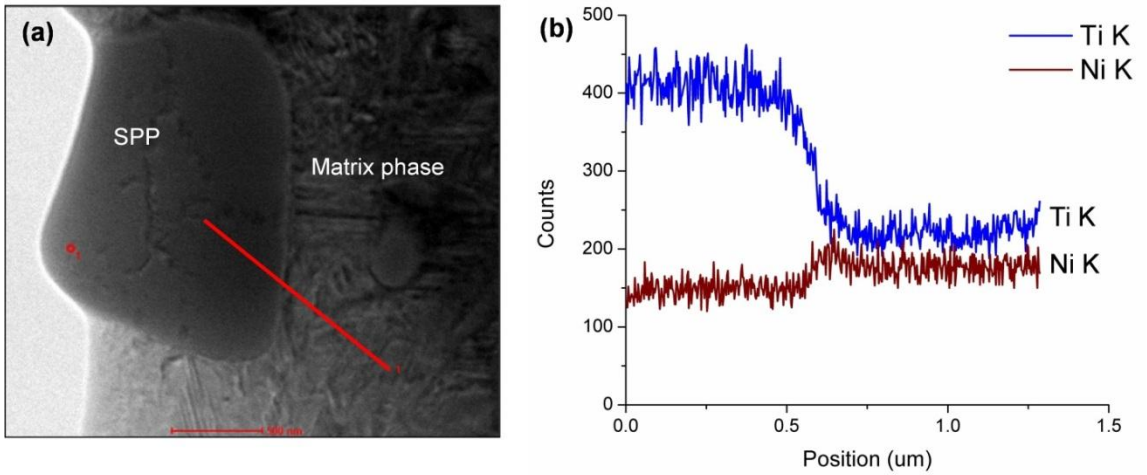

Figure 2 (a) STEM bright field image showing a SPP at the edge of thin foil, marked by a red spot,and (b) EDS composition profile along the line shown in (a).

Table 2 Composition analysis of matrix and second phase particle shown in Fig. 2(a)

Element	Matrix phase	Second phase particle
Ti	50.1± 0.2	66.7 ± 0.2
Ni	49.7± 0.2	33.3± 0.2

Microstructural features in matrix phase surrounding the Ti_2Ni SPP is shown in Fig.3 and Fig.4. Preferential nucleation of martensite twins from facets of Ti_2Ni phase is clearly evident from the microstructure shown in Fig.4. Examination also revealed the elastic strain field in localized regions along the SPP-matrix interface (Fig.3). It is evident from the microstructure in Fig. 4(a) that the elastic strain field associated with precipitation of Ti_2Ni phase has influence on formation of twins in martensite phase. Hence, it appears that the precipitation of Ti_2Ni phase during solidification could have acted as nucleation site for formation of martensitic twins. This is in accordance with the findings of Lopez et al. [18] wherein it has been reported that the Ti_2Ni particles in the microstructure act as preferential nucleation sites for martensite plates.

Figure 4(b) shows a typical microstructure of matrix phase away from Ti_2Ni particles. It shows twinned martensite grains as well as partially transformed martensite grains. From the phase diagram, it is expected that during solidification of binary NiTi alloys, Ti_2Ni phase forms through a peritectic reaction, $\beta + L \rightarrow \delta$ (Ti_2Ni), at 948°C [12,19].Formation of Ti_2Ni phase during solidification has been reported for both equi-atomic and Ti-rich NiTi alloys [11]. The cooling rate during solidification plays an important role on type of phase formed and their volume fraction in cast microstructure. It has been reported [20] that higher cooling rates result in formation of large amount of Ti_2Ni phase and thereby the matrix phase becomes Ti-lean. This shifts the transformation temperatures to lower side and hence, the cast structure contains significant volume fraction of austenite at room temperature. On the other hand, slow cooling results in formation of less volume fraction of Ti_2Ni phase and a homogeneous single phase martensitic structure. In the present case, the cooling rate was high in water cooled copper crucible and hence, the cast alloy is expected to contain SPPs and certain volume fraction of austenite phase, in addition to martensite phase (Fig. 4).

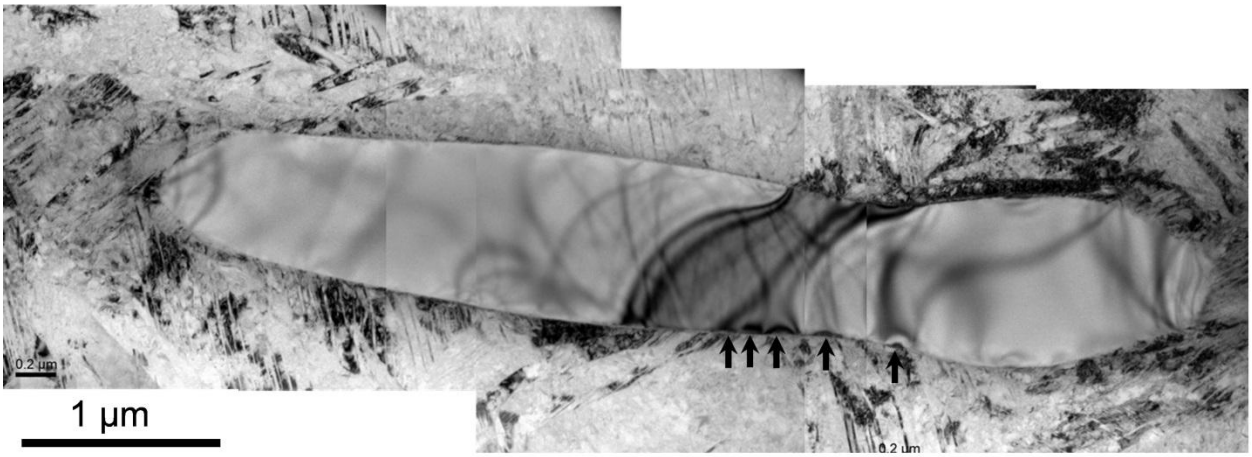

Figure 3 Montage of TEM micrographs of cast NiTi alloy showing a Ti_2Ni particle with high aspect ratio. The elastic strain field in localized regions of SPP-matrix interface is marked by arrows.

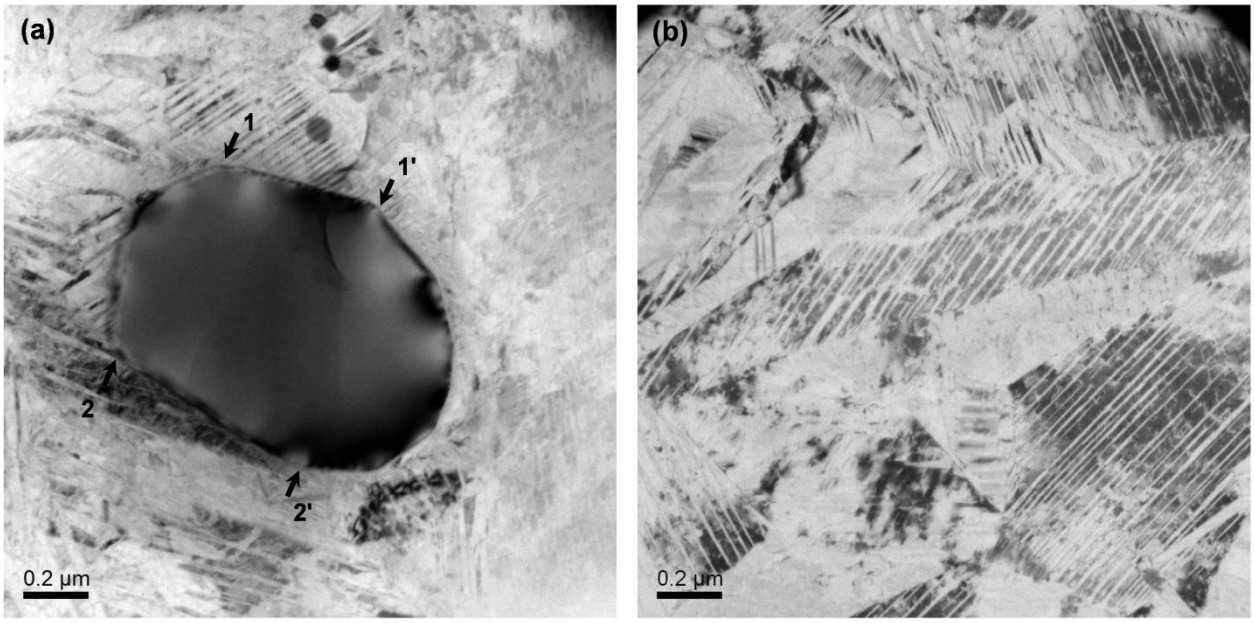

Figure 4 TEM micrographs showing microstructural details of (a) SPP-matrix interface, (b) away from SPP-matrix interface.

3.2 Behaviour of Ti_2Ni phase during hot rolling

The as-cast alloy was thermo-mechanically processed at 850°Cand the cross section of the sample was reduced by ~70% through groove rolling process in multiple steps (Table 1). Samples collected at various stages of hot working were quenched in water following by deformation process and were subjected to microstructural study. Figures 5 and 6 show the microstructures of specimens HR30 and HR70, respectively. It can be seen that the morphology of Ti_2Ni phase in terms of size, shape and distribution keeps changing significantly during hot deformation process.

Comparison of microstructures of as-cast alloy (Fig.1(a)) and sample HR30 (Fig.5(a)) shows that there is a substantial reduction in size of martensite grains/variants with hot deformation as low as 30%. Also, the variants are more randomly oriented in the hot deformed sample compared to that of the as-cast structure. The Ti_2Ni particles were found to be still located at the grain boundaries without any noticeable change in their size (Fig.5(b)). However, TEM micrograph showed that the SPPs were mostly oriented in the direction of rolling. Figure 5(c) shows a bright field TEM image of an ellipsoidal Ti_2Ni particle with major axis aligned along the rolling direction. Also, the matrix phase adjacent to the SPPs showed banded microstructure with multi-variant twinned martensite phase. With the progress of hot deformation process, the SPPs got elongated in the direction of rolling and after about 70% deformation, the elongated particles fragmented into many smaller particles (Fig.6). After fragmentation, the shape of the particles varied from slightly non-spherical to fairly spherical.

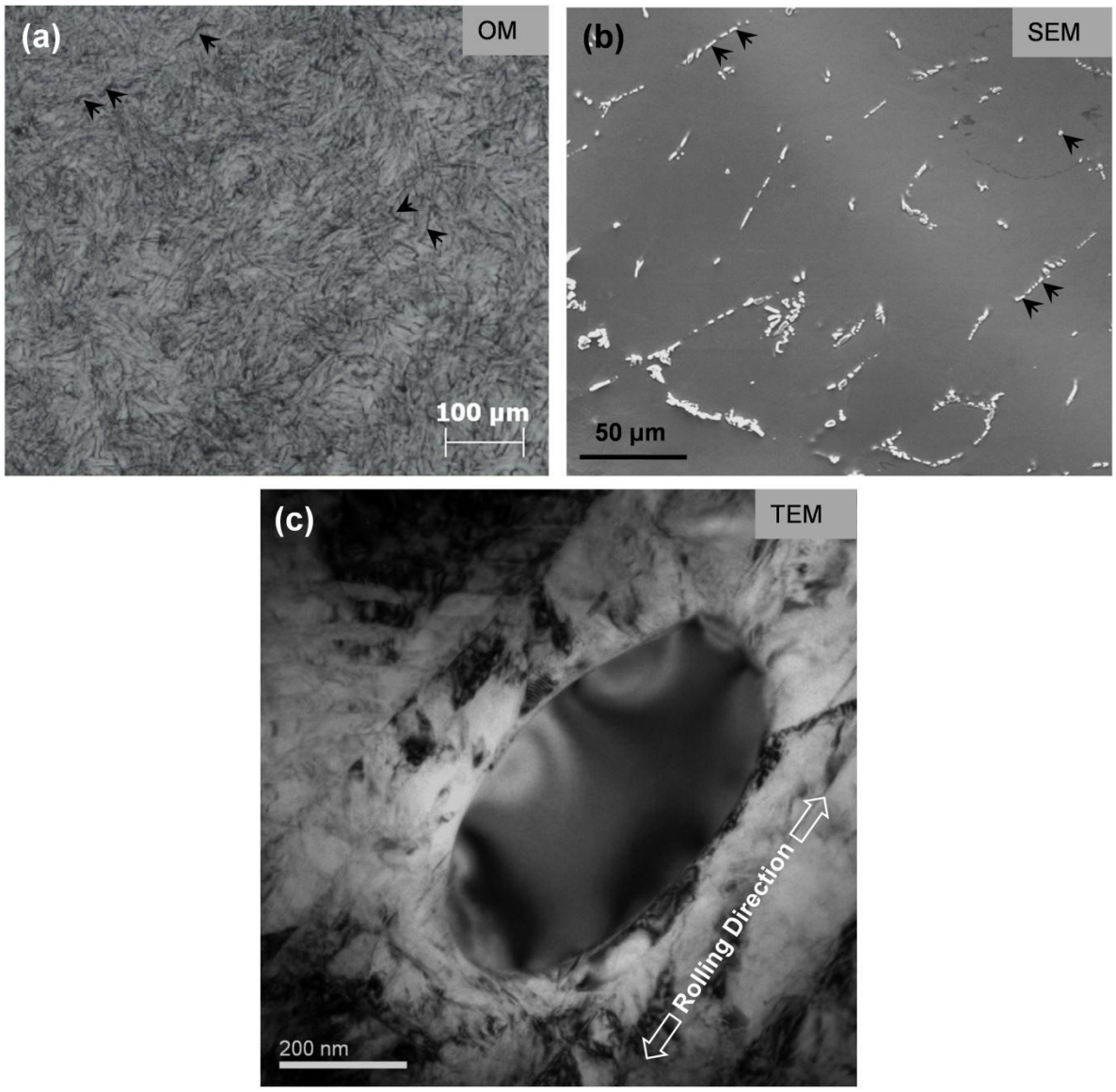

Figure 5 Microstructure of hot deformed sample after 30% reduction in cross section (HR30): (a) Optical micrograph, (b) SEM micrograph, and (c) TEM bright field micrograph.

Based on many observations on the SPP-matrix interfaces in many regions and more than one sample it is inferred that there was no separation/decohesion at the interface of matrix and SPPs during hot deformation. This indicates that Ti_2Ni phase is ductile enough at the hot working temperature so that the flow compatibility of matrix-SPP as a whole is maintained. However, based on the microstructural observations, the following hypothesis can be proposed on the behaviour of Ti_2Ni particles during hot deformation process. In the initial stages of hot working, along with the matrix phase, the Ti_2Ni particles also get deformed and elongated in the direction of rolling. After sufficient elongation, necking takes place at several locations along the length of the particle. Finally, shearing takes place at the constricted regions of the particle giving rise to fragmentation of the larger particle into a number of smaller particles. Such a process of fragmentation is evident from the TEM microstructure shown in Fig. 6(a). Another interesting observation found in a number of SPPs is illustrated in Fig. 6(b). This is typical of recrystallized microstructure of deformed and annealed materials. A group of SPPs are seen which can be thought of as a single SPP of about 1µm (before hot deformation) which got transformed into a group of sub-micrometer sizes contiguous grains as a consequence of dynamic recrystallization during thermomechanical processing at 850°C. Referring to the phase diagram, the processing temperature is close to peritectic transition temperature at which Ti_2Ni phase formed. It is possible that the deformation strain builds up in the particle with the accumulation of dislocations within and leads to dynamic recovery and recrystallization. This characteristic is seen associated with SPPs which show a more rounded-off morphology. The resulting grain boundaries here are high angle boundaries in contrast to the elongated SPPs which gets sheared and fragmented. This observation confirms the active participation of the Ti_2Ni phase during the hot deformation processing.

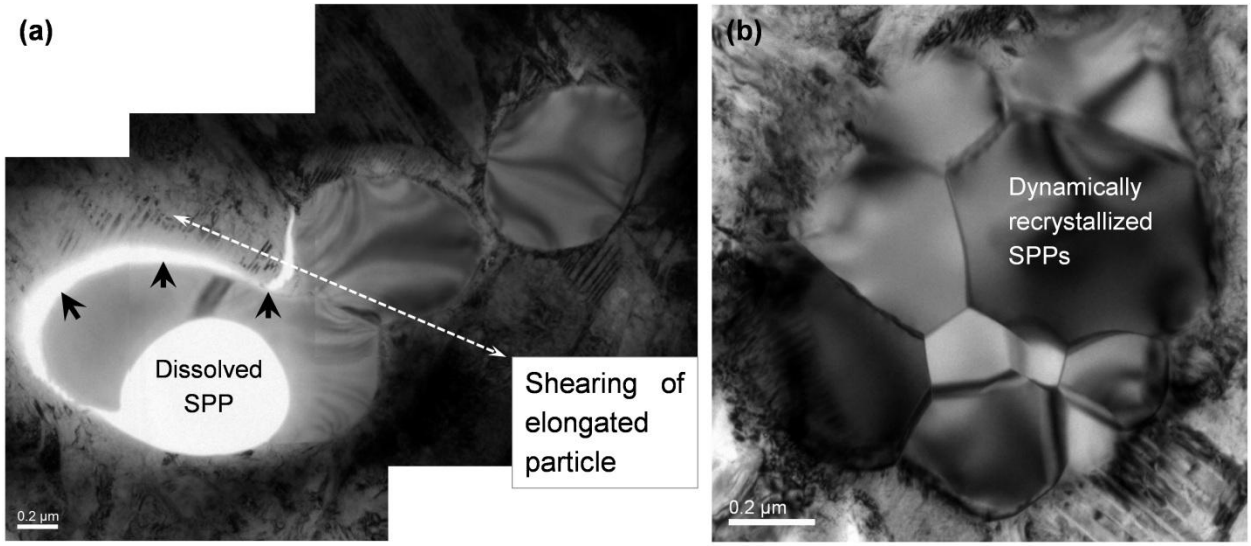

Figure 6 Microstructure of hot deformed sample after 70% reduction in cross-section (HR70) showing the deformation behaviour of Ti_2Ni SPP: (a) Necking and shearing of an elongated particle; and (b) ASPP experienced severe plastic deformation and dynamically recrystallized during hot rolling.

3.3 Behaviour of Ti_2Ni phase during cold rolling

The cross section of hot deformed rod (HR70) was further reduced by cold rolling in multiple steps with inter-pass annealing at 750°C for 10 min. Two samples CR80 and CR95 after 80 and 95% of cumulative cold deformation, respectively, were subjected to microstructural study. Figure 7 shows the SEM micrographs of these samples. It can be seen that cold rolling resulted in separation of the fragmented particles and are present in the form of stringers along the direction of rolling. The deformability of SPPs at ambient temperature was found to be relatively low compared to that at high temperature. This has resulted, not only in fracturing of the SPPs during cold deformation, but also separation of interface between the SPPs and the matrix phase (Fig. 7(b)). The dark regions close to SPPs in Fig. 7b and 7d, the SEM BSE images, are the opened up cracks. It has to be noted that the actual size of these cracks may be smaller than seen in these images as they could have grown slightly bigger during the electro-polishing for sample preparation. The fracturing of the SPPs was predominant at the early stage of cold deformation and hence, the particles are found irregular in shape. After fragmentation to certain size range, there was marginal reduction in size of the SPPs with the progress of cold deformation. Subsequently, during cold deformation and inter-pass annealing, morphology of SPPs changed to nearly round shape from irregular shape with the loss of sharp edges (Fig.7(d)).

Figure 8 shows the TEM microstructure of sample CR80. Figure 8(a) shows a group of four Ti_2Ni particles and the matrix phase surrounding these particles. At the right bottom corner of the micrograph and around the larger particle, a featureless region can be observed in the matrix phase. Selected area diffraction (SADP) from the region shown on Fig.8(a) by the dotted line circle is reproduced in Fig.8b. Pattern analysis confirmed that these featureless regions are predominantly amorphous in nature. Similar featureless matrix phase surrounding a cracked Ti_2Ni particle is depicted in Fig.8(c). A few more illustrations of material flow characteristics around matrix phase surrounding the SPPs are depicted in Figs.8(d-e) and a possible flow pattern has been shown by a series of arrows in Fig.8(d). It is clear from these TEM images that during cold working, the deformability of the matrix phase is significant and the SPP remains virtually undeformed. Role of non-deformable SPPs in FCC alloy systems has been well studied. Humpherys [14,15] considered lattice rotations at SPPs of varying sizes in Al and Cu single crystals. Based on SADP analysis, it has been shown that there are large scale lattice rotations of up to 30-40° around specific crystallographic directions. Alternative mechanisms to explain lattice rotations around SPPs based on continuum approach have been suggested by Ashby [21] and Brown and Stobbs [22]. Non-deformable particles of size >1μm only are shown to be effective in large scale shear strains and the consequent lattice rotations. Apps et al.[16] studied the effect of SPPs on the rate of grain refinement during severe deformation processing using equal channel angular pressing (ECAP) and characterization by electron back scattered diffraction (EBSD). It was shown that particle containing alloys required much fewer numbers of passes to get sub-micrometer sized grains compared to the single phase alloys. Extending similar arguments to the present case, there exist a region surrounding the SPPs where material flow by shear deformation is very severe resembling the conditions that exist in severe plastic deformation processing of metallic materials. Amorphisation in NiTi system and subsequent nanometer scale martensite phase formation has been demonstrated by Waitz et al. [23] through TEM studies on high pressure torsion (HPT) processed material.

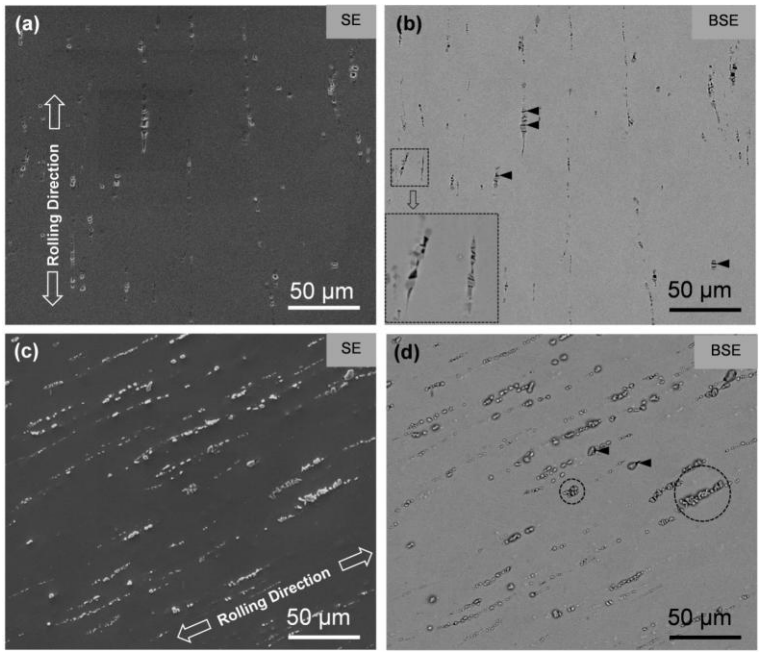

Figure 7 SEM micrographs of cold deformed sample showing distribution of SPPs and their morphology: (a) Secondary electron (SE) image and(b) back scattered electron (BSE) image of sample CR80, (c) SE image and (d) BSE image of sample CR95. Arrows in (b) and (d) indicate opened up cracks close to SPP fragments.

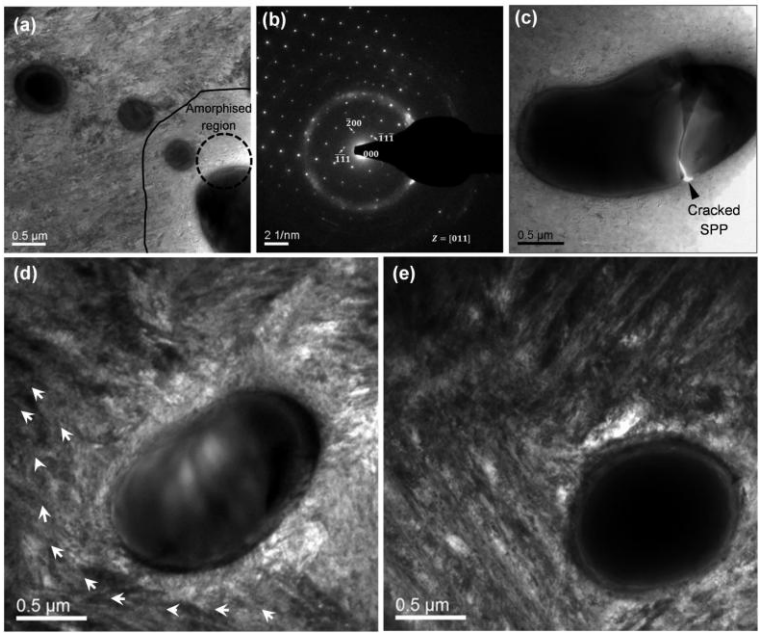

Figure 8 TEM micrographs of sample CR80: (a) Group of four particles showing featureless matrix phase surrounding the particle at the bottom right corner; (b)SADP from region encircled in (a) by dotted line; (c) A cracked/fragmented SPP and featureless (amorphous) matrix phase, and (d)-(e) More illustrative examples material flow characteristics surrounding SPPs.

Figure 9 shows bright field TEM micrographs of 95% cold rolled sample (CR95) illustrating the microstructural features of matrix phase around a SPP. The material was found to contain a very high density of dislocations. The SADP taken in this region confirmed that the matrix phase contained a mixture of both austenite and martensite phases (Fig.9(c-d)). Close observation of the micrograph shows strong contrast regions typical of recovered microstructure of severely deformed materials. This observation is suggestive of formation of fairly recovered structure in localized regions around SPPs. The arced nature of the spots in the SADP indicates micro-texture resulting in the matrix region around SPPs. These observations can be considered to provide direct evidence to the possibility that during cold deformation of NiTi sufficient heat is generated in the sample which in turn, induces dynamic recovery of microstructure. This phenomenon was found to be more prominent in the matrix phase regions surrounding the SPPs rather than those away from the SPPs (Fig.9(a)).The possibility of heat generation within the samples during cold working and the consequential formation of strain induced B2 phase during cold deformation of Ti-rich NiTi have been reported by Lopez et al [18].

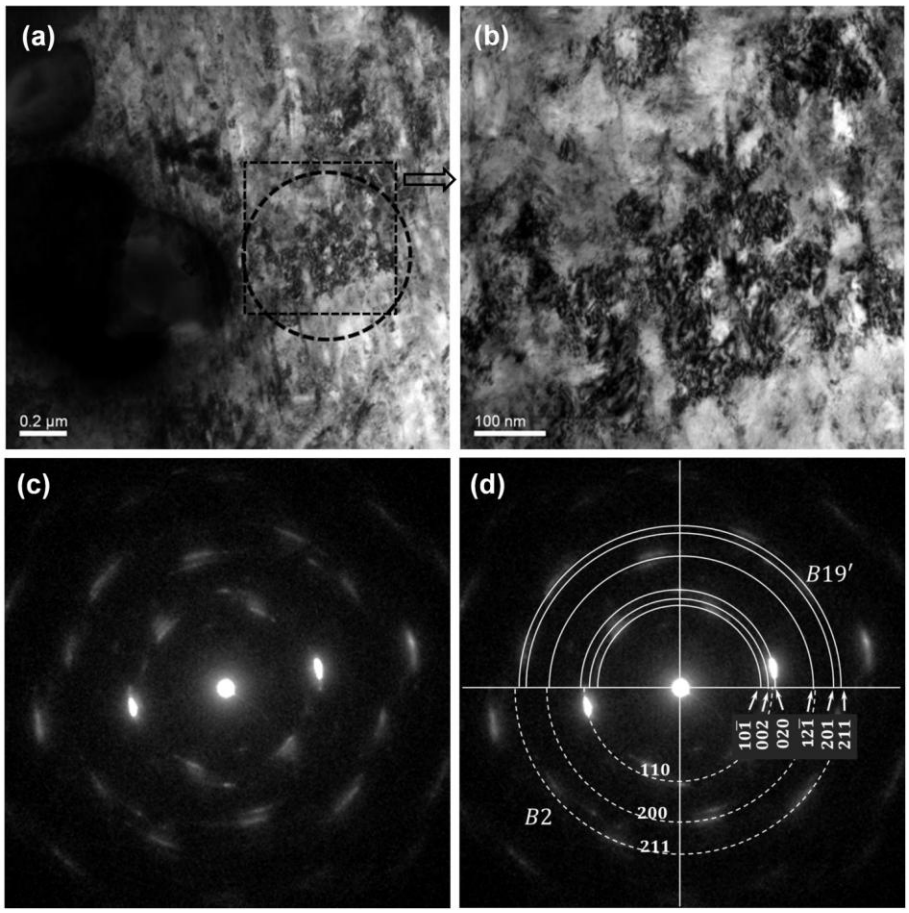

Figure 9 TEM bright field images of sample CR95 showing: (a) Dynamically recovered structure close to a SPP, (b) Higher magnification image of the region in the box shown on (a), (c) SADP of the matrix phase in the vicinity of SPP shown by dotted line circle in (a), and (d) indexed SADP shown in (c) with dotted line indicating the position of B2 phase reflections and solid lines indicating that of B19'.

3.4 Role of Ti_2Ni on microstructural refinement during wire drawing

The cold rolled sample (CR95) was annealed and subjected to multiple step cold wire drawing process to obtain a wire of diameter500 μm. The microstructure of the cold drawn wire with 40% reduction in cross section (sample: CDW40) is shown in Fig.10. The flow of matrix phase surrounding a typicalTi_2Ni particle is shown by a series of arrows in Fig.10(a). Although, the overall deformation pattern in the matrix phase surrounding the SPPs was similar to that described in Section 3.3 (compare Fig.8(d) and Fig.10(a)), the flow behaviour, however, is found to be dependent on the size and shape of the SPPs. In case of relatively smaller particle, the shear deformation in the matrix phase was mostly confined close to the SPP-matrix interface while, this deformation zone was found to be extended in case of larger SPPs (Fig. 10(a)).

The SADP shown in Fig. 10(b) was obtained from a region comprising of SPP and severely deformed matrix phase. The broad diffuse halos in the SADP clearly indicate amorphisation of matrix around SPP. In addition, the SADP shows strong systematic array of diffracted spots corresponding to Ti_2Ni phase. The fine spots making discontinuous rings of intensities indicate

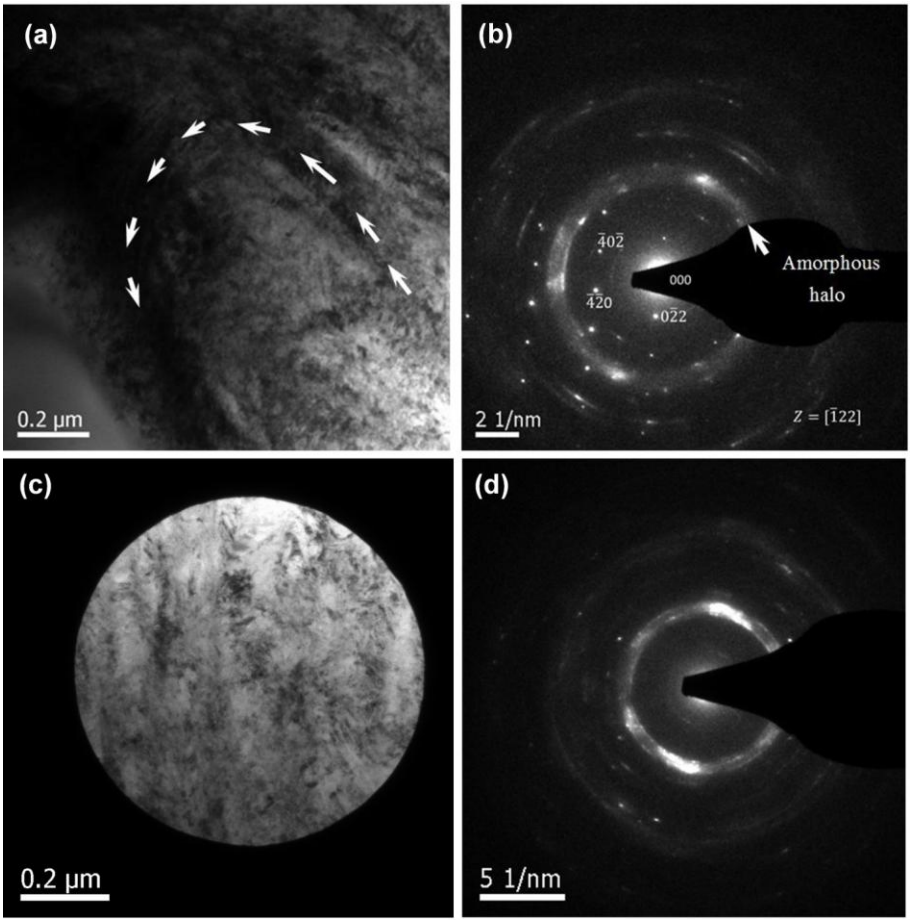

Figure 10 TEM microstructure of cold drawn wire with 40% retained cold work (sample:CDW40):(a)Flow of matrix around a typical Ti_2Ni particle; (b) SADP of the SPP-matrix overlapped region shown in (a), (c) bright field image away from SPP, and (d) SADP of the region shown in (c).

presence of phases such as austenite, martensite and possibly R-phase. Figure 10(c)shows the TEM bright filed micrograph representing the typical microstructural characteristics of matrix phase away from SPP. The SADP from this region is shown in Fig. 10(d).The diffuse halos confirm significant degree of amorphisation in the matrix phase. The strong intensity arcs (indicated by arrows in Fig. 10(d)) signify preferred directionality of deformations and the consequent presence of texture in the crystalline (nano-crystallites) fraction of the matrix phase. In the SADP, the fine spots, forming discontinuous rings, are from other co-existing phases that are present in the material in nanometer scale. Based on these observations it can be inferred that the microstructural refinement in the matrix phase is stronger near to the SPPs than the regions away from Ti_2Ni particles. This leads to a non-uniform microstructure. Consequence of this type of microstructure will be difference in response to annealing treatment and hence possible development of a bimodal size distribution of crystallites/variants. Such a microstructural distribution is expected to play different and critical role in determining the functional characteristics of the SMA wire.

Conclusions

The following conclusions can be drawn from the present study on the behavior of Ti_2Ni and its effect on the microstructural evolution in vacuum arc-melted 50.2Ti-Ni (at.%) alloy during processing of the alloy into wire form.

1. Slightly Ti-rich NiTi alloy contained about 1-2% (by volume) of Ti_2Ni second phase particles(SPPs) in the microstructure. In as-cast alloy, the Ti_2Ni particles are present in varying sizes (1-10 μm) and shapes.
2. During subsequent thermo-mechanical processing, the Ti_2Ni SPPs get sheared/fragmented into smaller particles and tend toward becoming more equiaxed.
3. The SPPs retain to a fair extent good orientation relationship across the interface with matrix, both in as-cast and worked condition and hence can help nucleation of martensite grains/variant.
4. During hot and cold deformation of alloy, the matrix phase surrounding the SPPs undergoes severe plastic deformation leading to amorphisation of the matrix and its localized recovery of structure.
5. The SPPs in the microstructure play a significant role in the formation of a non-uniform non-equilibrium microstructure.

Acknowledgements

The work presented in this paper was carried out with the financial support under National Programme on Micro and Smart Systems (Grant No. NPMaSS:Proj.San:PARC#1:3), Aeronautical Development Agency (ADA), DRDO, Bangalore, India.

REFERENCES

[1] M. Schwartz, Encyclopedia of smart materials, John-Wiley, New York, 2002.

[2] K. Otsuka, C.M. Wayman, Shape memory materials, Cambridge University, 1998.

[3] T.W. Duerig, K.N. Melton, D. Stockel, C.M. Wayman, Engineering aspects of shape memory alloys, Butterworth- Heinemann, London, 1990.

[4] K. Otsuka, X. Ren, Physical metallurgy of Ti-Ni based shape memory alloys, Prog. Mater. Sci., 50 (2005) 511-678.

[5] R.J. Wasilewski, S.R. Butler, J.E. Hanlon, D. Worden, Homogeneity range and the martensitic transformation in TiNi, Metall. Trans., 2 (1971) 229-238.

[6] K. Melton, O. Mercier, The mechanical properties of NiTi-based shape memory alloys, Acta metall., 29 (1981) 393-398.

[7] S. Miyazaki, K. otsuka, Y. Suzuki, Transformation pseudoelasticity and deformation behavior in Ti-50.6at%Ni alloy, Scripta Metall. 15 (1981) 287-292.

[8] S. Miyazaki, K. Otsuka, Deformation and transition behavior associated with the R-phase in Ti-Ni alloys, Metall. Mater. Trans. A, 17 (1986) 53-63.

[9] W. Tang, Thermodynamic study of the low-temperature phase B19' and the martensitic transformation in near-equiatomic Ti-Ni shape memory alloys, Metall. Mater. Trans. A, 28 (1997) 537-544.

[10] M. Nishida, C.M. Wayman, T. Honma, Precipitation processes in near-equiatomic TiNi shape memory alloys, Metall. Trans. A, 17 (1986) 1505-1515.

[11] S. P. Gupta, K. Mukherjee, A. A. Johnson, Diffusion controlled solid state transformation in the near equiatomic Ti-Ni alloys, Mater. Sci. Eng., 11 (1973) 283-297.

[12] H.F. Lopez, A. Salinas-Rodriguez, J. L. Rodriguez-Galicia, Microstructural aspects of precipitation and martensitic transformation in a Ti-rich Ni-Ti alloy, Scripta Mater., 34 (1996) 659-664.

[13] L. M. Wu, S. K. Wu, The evolution of Ti_2Ni precipitates in annealed $Ti_{51}Ni_{49}$ shape memory melt spun ribbons, Phil. Mag. Lett., 90 (2010) 261-268.

[14] F.J. Humphreys, The nucleation of recrystallization at second phase particles in deformed aluminium, Acta Metall., 25 (1977) 1323-1344.

[15] F.J. Humphreys, Local lattice rotations at second phase particles in deformed metals, Acta Metall., 27 (1979) 1801-1814.

[16] P.J. Apps, J. R. Bowen, P.B. Pragnell, The effect of coarse second-phase particles on the rate of grain refinement during severe deformation processing, Acta Mater., 51 (2003) 2811-2822.

[17] F.J. Humphreys, M. Hatherly, Recrystallization and related annealing phenomena, second edition, Elsevier, Oxford, 2004.

[18] H. F. Lopez, A. Salinas, H. Calderon, Plastic straining effects on the microstructure of a Ti-rich NiTi shape memory alloy, Metall. Mater. Trans. A, 32 (2001) 717-729.

[19] T.B. Massalski, H. Okamoto, P.R. Subramanian, L. Kacprzak (Eds.), Binary Alloy Phase Diagrams, 2nd edition, Vol. 3. Materials Park, OH: ASM International, 1990, p. 2874.

[20] M. Their, M. Huhner, E. Kobus, D. Drescher, C. Bourauel, Microstructure of as-cast TiNi alloy, Mater. Char., 27 (1991) 133-140.

[21] M. F. Ashby. Work hardening of dispersion hardened crystals, Philos. Mag, 14 (1966) 1157-1178.

[22] L. M. Brown , W. M. Stobbs. The work hardening of copper silica, Philos. Mag, 23 (1971) 1201-1233.

[23] T. Waitz, V. Kazykhanov, H.P. Karnthaler, Martensitic phase transformations in nanocrystalline NiTi studied by TEM, Acta. Mater., 52 (2004) 137-147.